Est. 1984

ORIENTAL JOURNAL OF CHEMISTRY
An International Open Access, Peer Reviewed Research Journal

www.orientjchem.org

ISSN: 0970-020 X
CODEN: OJCHEG
2020, Vol. 36, No.(5):
Pg. 825-833

Structural, Vibrational, Electronic and Optical Properties of 3-methoxy-2,4,5-trifluorobenzoic Acid Using DFT Calculations

S. JEYAVIJAYAN[1]* and PALANI MURUGAN[2]

[1]Department of Physics, Kalasalingam Academy of Research and Education,
Krishnankoil-626 126, Tamil Nadu, India.
[2]Department of Physics, Dr. B.R. Ambedkar Institute of Technology,
Port Blair-744103, Andaman & Nicobar Islands, India.
*Corresponding author E-mail: sjeyavijayan@gmail.com

http://dx.doi.org/10.13005/ojc/360505

(Received: July 22, 2020; Accepted: October 04, 2020)

ABSTRACT

The molecular vibrations of 3-methoxy-2,4,5-trifluorobenzoic acid (MFBA) were studied by recording the FTIR and FT-Raman spectra and the vibrational frequencies have been compared with the DFT-B3LYP calculations. The optimized structural characteristics of the molecule have been studied by both calculated and experimental data. NBO analyses and the LUMO-HOMO energy gap of the molecule shows the intramolecular charge transfer interaction. Further, the nonlinear optical properties of MFBA have been investigated from the calculated values of first hyperpolarizability and total dipolemoment. The electrostatic potential and Mulliken charges of MFBA have also been performed.

Keywords: FT-Raman, FTIR; 3-methoxy-2,4,5-trifluorobenzoic acid, DFT calculations; NLO.

INTRODUCTION

Benzoic acid is the standard chemical used in bomb calorimeter to determine the heat capacity. Benzoic acid enhances the growth of mold, yeast, bacteria. Skin diseases are treated by benzoic acid[1]. Topical antiseptics and inhalant decongestants products are mainly based on benzoic acid derivatives. Further, in food preservatives[2] salts of benzoic acids utilized. Benzoic acid derivatives are also used to diagnosis gastrointestinal complaints and fibrotic skin disorders[3] to protect from UV radiation. The chemical and pharmaceutical industries prepare substituted benzoic acids by the oxidation of corresponding substituted toluene[4]. From the patent report, it reveals that benzoic acids selectively control the tumor tissue[5]. The interesting features in spectroscopic area of benzoic acids and their derivatives have been already studied by many researchers[6,7]. Hence, owing to the important and significant features of substituted benzoic acids, a detailed study on spectroscopic research of 3-methoxy-2,4,5-trifluorobenzoic acid (MFBA) was carried out.

More exact structure and wavenumbers of polyatomic molecules can be predicted from the

density functional theory (DFT) methods and they are superior prediction than the ab initio calculations[8]. The DFT approach for determining the various molecular properties are powerful tool and being routinely used. Large and medium size molecule can be described by B3LYP functional which offer an outstanding concession between computational efficiency and accuracy of vibrational band spectra[9,10]. Therefore, the DFT-B3LYP method is the greatest in calculating molecular geometry and vibrational bands even for bigger molecular structure.

EXPERIMENTAL

A pure sample of polycrystalline MFBA procured and used for spectral measurements. JASCO FTIR-6300 spectrometer instrument have been utilized for recording the title molecule to get FT-IR spectrum at normal temperature for wave number 4000-400 cm^{-1} with KBr pellet and FT-Raman spectra of MFBA recorded on a BRUKER/RFS-100/S model interferometer using accessories of FT-Raman (FRA-106) in Stokes region from 4000-50 cm^{-1} (for excitation 1064 nm wavelength line laser of Nd:YAG source of power 150 mW is used). The accuracy of $\pm$ 4 cm^{-1} is maintained.

Computational

DFT-B3LYP method[11] for MFBA with basis set of 6-311++G(d,p) were done using Gaussian 09W program package[12] to obtain molecular geometry optimization, electronic, optical and thermodynamic properties using Lee *et al.,*[13] correlation function. It is being ensured that the calculations were converged to a minimum value as the imaginary frequencies were absent. For that, the force constant illustrated by the Cartesian provide the complete geometry of optimization of MFBA. Further, the molecular parameters to describe the structure were employed to calculate frequencies. The force constants scaled by DFT scale factor of 0.9613 to get good contract with the data obtained from experiment by adopting SQM procedure[14]. The electronic and thermodynamic parameters of MFBA were calculated by the method B_3LYP. The total energy distribution (TED) percentages associated with each vibration are calculated with MOLVIB program[15].

RESULTS AND DISCUSSION

Molecular structure

Figure 1 shows the MFBA molecular structure. In the B3LYP-6-311++G(d,p) method, the energy calculated is -833.276940748 Hartrees for the MFBA molecule. Further, Table 1 represents the optimized geometrical parameters for MFBA together with the X-ray diffraction data[16,17] from experiment. As seen from the observation, the computed geometries from B3LYP method are consistent with the observed values for MFBA. In the B3LYP calculation, it's been clearly observed that, the regular benzene ring distorted slightly because of the influence of substituent groups in the ring system. The COOH, methoxy groups and fluorine atoms in the position of H atoms slightly change the bond angle from the prefect planner structure. Due to the C4–C3, C3-C2, C1–C2 bond lengths and C5–C4 at the substitution place, the ring looks to be imbalanced, which are calculated values as 1.397, 1.398, 1.393 and 1.392 Å, respectively (1.396, 1.393, 1.390 and 1.391 Å by experimental[14]). In MFBA ring, the lengths of the bond are smaller than C1-C6 bond length. In the DFT calculations, the bond angles of C6–C1–C2, C3–C2–C1, C4–C3–C2, C5–C4–C3 and C6–C5–C4 are found as 117.69°, 123.44°, 116.89°, 120.82° and 120.92°, respectively, (Experimental values: 120.52°, 119.62°, 120.31°, 119.34° and 121.13°). These are deviated from regular 120° and this irregularity of the angles explains the significance of the repulsion between COOH, methoxy groups, fluorine atoms and the ring system.

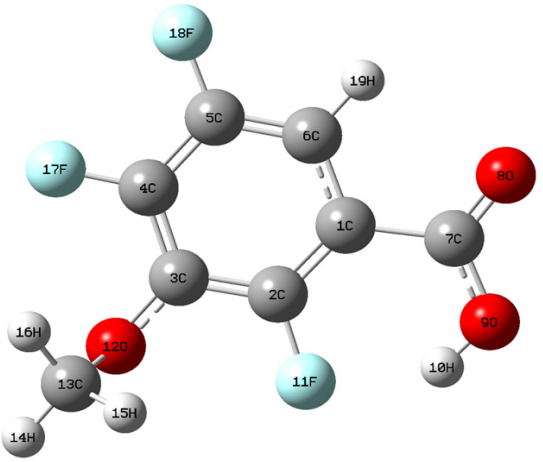

Fig. 1. Structure of 3-methoxy-2,4,5-trifluorobenzoic acid

Table 1: Geometrical optimized parameters for 3-methoxy-2,4,5-trifluorobenzoic acid

Bond length	Value (Å) B3LYP-6-311++G(d,p)	[16,17]Expt	Bond angle	Value (°) B3LYP-6-311++G(d,p)	[16,17]Expt
R(1,2)	1.393	1.390	A(2,1,6)	117.69	120.52
R(1,6)	1.401	1.402	A(2,1,7)	125.97	120.47
R(1,7)	1.511	1.482	A(6,1,7)	116.34	119.01
R(2,3)	1.398	1.393	A(1,2,3)	123.44	119.62
R(2,11)	1.360	1.343	A(1,2,11)	120.21	118.93
R(3,4)	1.397	1.396	A(3,2,11)	116.35	117.35
R(3,12)	1.354	1.367	A(2,3,4)	116.89	120.31
R(4,5)	1.392	1.391	A(2,3,12)	119.81	115.43
R(4,17)	1.339	1.337	A(4,3,12)	123.17	124.26
R(5,6)	1.378	1.383	A(3,4,5)	120.82	119.34
R(5,18)	1.343	1.349	A(3,4,17)	119.49	117.98
R(6,19)	1.082	0.950	A(5,4,17)	119.69	118.13
R(7,8)	1.202	1.239	A(4,5,6)	120.92	121.13
R(7,9)	1.347	1.311	A(4,5,18)	118.42	117.62
R(9,10)	0.967	1.010	A(6,5,18)	120.66	118.69
R(12,13)	1.442	1.430	A(1,6,5)	120.24	119.09
R(13,14)	1.091	0.980	A(1,6,19)	119.05	120.2
R(13,15)	1.088	0.980	A(5,6,19)	120.71	120.2
R(13,16)	1.093	0.980	A(1,7,8)	121.27	121.76
			A(1,7,9)	118.29	115.39
–	–	–	A(8,7,9)	120.44	122.85
–	–	–	A(7,9,10)	111.87	109.8
–	–	–	A(3,12,13)	117.02	116.94
–	–	–	A(12,13,14)	111.21	109.5
–	–	–	A(12,13,15)	105.42	109.5
–	–	–	A(12,13,16)	110.18	109.5
–	–	–	A(14,13,15)	109.85	109.5
–	–	–	A(14,13,16)	110.34	109.5
–	–	–	A(15,13,16)	109.73	109.5

Vibrational assignments

There are 19 atoms in the investigated molecule. From the structure, the C1 point group symmetry is possessed by MFBA and there are 51 vibrational modes. Based on the theoretical prediction and recorded spectra of FT-IR and FT-Raman, the wave numbers of the vibrational assignments are presented in Table 2. The Fig. 2 represents FT-IR and Fig. 3 represents FT-Raman spectra of MFBA. The experimental frequencies are less than the computational values due to combination of correlation effects of electron and deficiencies in the basis set method. However, they are agreed on inclusion of the scaling factors.

C-H vibrations

The regions between 3100-3000 cm^{-1} are generally found as typical region for C-H stretching vibration[18]. In MFBA, scaled B3LYP-6-311++G(d,p) computed wavenumbers in 3092 cm^{-1} represents C-H stretching mode of vibrations (97% TED). Similarly, the experimental values of both IR band and Raman band are noticed at 3087 cm^{-1}. The C-H in-plane and C-H out-of-plane vibrations in MFBA seemed to be in coincidence with the calculated wave numbers as identified in Table 2.

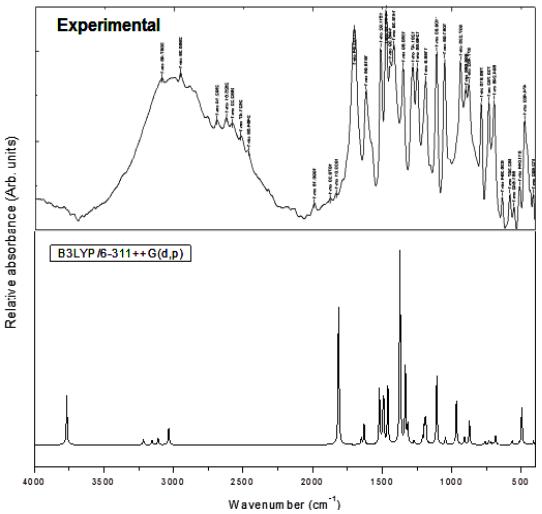

Fig. 2. Calculated and observed FTIR spectra of 3-methoxy-2,4,5-trifluorobenzoic acid

Table 2: Observed and calculated wavenumbers of 3-methoxy-2,4,5-trifluorobenzoic acid

Sl.No.	Observed wavenumber (cm^{-1})	Calculated wavenumber (cm^{-1}) B3LYP/6-311++G(d,p)							Assignment (TED %)
	FTIR	FT-Raman	Unscaled	Scaled	Reduced mass	Force Constant	IR intensity	Raman activity	
1	3452(vs)	-	3767	3621	6.14	13.46	91.91	1.10	νOH (99)
2	3087(vs)	3087(ms)	3216	3092	5.61	23.76	241.52	1.04	νCH (97)
3	2955(ms)	2958(s)	3152	3030	17.83	415.80	143.27	9.57	CH_3 ips (95)
4	2850(vw)	2886(w)	3110	2990	9.21	3.88	148.64	1.10	CH_3 ss (94)
5	2832(vw)	2845(ms)	3033	2916	8.94	164.89	144.05	4.66	CH_3 ops (92)
6	1703(vs)	-	1814	1744	6.64	342.69	85.03	8.07	νC=O (89)
7	-	1674(s)	1650	1586	6.54	0.99	57.01	3.30	νCC (87)
8	1619(s)	1622(vs)	1630	1567	6.39	2.24	113.67	3.18	νCC (85)
9	1512(vs)	-	1520	1461	6.70	159.54	56.75	5.63	νCC (83)
10	-	1512(ms)	1504	1446	9.75	94.40	3.73	1.62	νCC (80)
11	1473(vs)	1464(vw)	1494	1436	9.63	117.07	23.59	4.42	νCC (79)
12	-	1459(ms)	1490	1432	3.63	85.32	30.74	5.47	νCC (78)
13	1445(w)	1434(w)	1460	1403	1.73	8.09	9.99	4.81	νCC (79)
14	1418(ms)	-	1373	1320	1.35	6.70	0.91	3.77	CH_3 ipb (79)
15	1350(s)	1355(vs)	1334	1282	3.58	69.39	21.23	5.45	CH_3 sb (77)
16	1281(s)	-	1317	1266	1.49	143.81	2.43	1.31	νCF(72)
17	-	1279(ms)	1272	1223	3.75	9.96	8.56	1.40	bOH (74)
18	1250(s)	1250(vw)	1211	1164	2.88	60.62	13.49	5.41	νCF(72)
19	1189(s)	-	1197	1151	0.70	12.44	0.04	1.88	νCF(72)
20	-	1169(ms)	1187	1141	0.73	11.33	0.05	3.02	νCO (78)
21	-	1125(vw)	1168	1123	2.74	43.91	9.94	5.13	νCO (79)
22	1109(vs)	1116(ms)	1108	1065	1.57	47.12	4.93	1.72	νCO (77)
23	1052(vs)	1055(ms)	1046	1006	3.43	1.88	17.64	4.64	bCH(74)
24	937(s)	939(s)	967	930	2.00	25.18	9.63	3.77	CH_3 opb (75)
25	899(ms)	898(ms)	909	874	1.03	8.29	11.79	1.23	bC=O (73)
26	877(ms)	-	874	840	1.42	7.99	0.43	9.19	CH_3 ipr (70)
27	786(s)	795(vw)	763	733	1.67	15.10	5.82	3.34	Rtrigd (69)
28	734(s)	745(vw)	734	706	0.69	0.05	2.44	1.31	Rasymd (71)
29	-	726(ms)	722	694	1.66	7.41	0.05	1.04	Rsymd (68)
30	694(s)	689(vs)	706	679	1.35	13.54	1.58	2.89	CH_3 opr (67)
31	-	660(vw)	685	658	1.49	1.62	1.26	1.25	bCO (71)
32	636(ms)	652(vw)	648	623	1.13	15.27	4.69	3.38	bCO (72)
33	582(ms)	584(w)	565	543	1.24	13.18	1.21	2.64	bCO (69)
34	511(ms)	516(s)	518	498	1.70	95.59	1.92	6.11	bCC (68)
35	474(s)	-	497	478	1.00	1.42	0.10	6.15	νOH (62)
36	-	469(vs)	471	453	0.94	8.92	1.16	2.61	ωCH (64)
37	412(w)	413(s)	414	398	0.32	49.19	1.69	1.54	νCC (60)
38	-	392(vw)	397	382	0.82	0.88	4.34	3.50	νC=O (59)
39	-	370(s)	380	365	0.94	6.05	0.48	2.20	tRsymd(58)
40	-	362(vw)	348	335	0.30	43.87	116.12	1.24	tRasymd (54)
41	-	318(vw)	334	321	0.36	30.09	22.82	1.73	tRtrigd(59)
42	-	284(vw)	302	290	0.50	1.00	0.39	2.19	bCF(58)
43	-	276(vw)	288	277	0.09	4.12	0.70	2.34	bCF(59)
44	-	245(ms)	230	221	0.67	6.27	1.42	1.50	bCF(60)
45	-	185(w)	200	192	0.18	0.91	0.24	1.56	ωCO(62)
46	-	157(vw)	170	163	0.17	82.21	0.04	1.09	ωCO(61)
47	-	134(vw)	144	138	0.07	103.93	16.69	1.09	ωCO(62)
48	-	112(vw)	114	110	0.11	0.87	0.23	1.10	ωCF(59)
49	-	91(s)	89	89	0.01	0.01	0.30	1.07	ωCF(58)
50	-	-	48	48	0.03	0.11	0.35	1.06	ωCF(57)
51	-	-	45	45	0.02	0.77	0.01	1.09	tCH_3 (54)

(ν) stretching, (ω) out-of-plane bending, (b) bending, (R) ring, (trigd) trigonal deformation, (asymd) antisymmetric deformation, (symd) symmetric deformation, (t) torsion, (ss) symmetric stretching, (ips) in-plane stretching,(ipr) in-plane rocking, (sb) symmetric bending,(ops) out-of-plane stretching, (opr) out-of-plane rocking, (w) weak, (vw) very weak, (vs) very strong,(s) strong,(ms) medium strong.

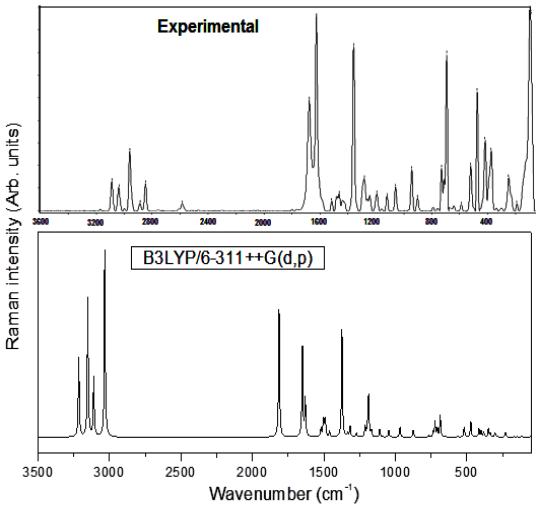

Fig. 3. Calculated and observed FT-Raman of 3-methoxy-2,4,5-trifluorobenzoic acid

CH_3 vibrations

In general, each CH_3 group can be associated with nine fundamentals. They are asymmetric CH_3 stretch, symmetric CH_3 stretch, in-plane CH_3-bending, in-plane CH_3 rocking, out-of-plane CH_3 stretch, out-of-plane CH_3 bending, out-of-plane CH_3 rocking, symmetric CH_3 bending and twisting CH_3 hydrogen mode. The donor electron substituent due to CH_3 group in the ring of aromatic compound is expected about 2870 and 2980 cm^{-1} for symmetric and antisymmetric stretching CH_3 modes[19], respectively. In CH_3 anti-symmetric stretching, one C–H bond is contracting and other two C–H bonds are expanding but in CH_3 symmetric stretching, it is found that all C–H bonds contract and expand in same phase. The scaled wavenumbers by B_3LYP method at 3030 cm^{-1} and also Raman and IR bands active at 2958 and 2955 cm^{-1} are CH_3 in-plane stretching mode with 95% contribution towards TED. The experimental modes obtained at 2880 and 2886 cm^{-1} and computed band at 2990 cm^{-1} concluded as symmetric CH_3 stretching of MFBA. In addition, the CH_3 deformation vibrations occur at 1390-1370 cm^{-1} and 1465-1440 cm^{-1} regions for symmetric and anti-symmetric respectively[20]. Thus, in MFBA, the IR band occurred at 1418 cm^{-1} is assigned to in-plane CH_3 bending vibration. The wavenumbers 1350 and 1355 cm^{-1} in the observed bands have been allocated to CH_3 symmetric bending modes. The other fundamental modes of CH_3 group vibration are in conformity with the calculated wave numbers by B3LYP method and are shown in Table 2.

COOH group vibrations

The characteristic feature of carboxylic group is detected at 1690-1655 cm^{-1} and is because of stretching of C=O vibration[21]. In MFBA, the computed band at 1744 cm^{-1} and IR band at 1703 cm^{-1} represents C=O stretching. The other two typical carboxylic group vibrations are known as: in plane O-H bending and C–O stretching[22]. Generally, C–O mode stretching occurs at 1350-1200 cm^{-1} range and hence wavenumber at 1169 cm^{-1} assigned to stretching C–O mode of MFBA. Hydrogen bonding in the ring system seems with band broadening[23], increased intensity and decreases the band regions to 3200–3550 cm^{-1}. Therefore, the IR wavenumber at 3452 cm^{-1} assigned for the stretching vibrations of OH group which is further confirmed by their TED (99%). Due to strong intermolecular interaction, the in-plane O-H bending vibration is commonly noticed in the 1440–1260 cm^{-1} region. Therefore, the Raman mode at 1279 cm^{-1} is assigned for the in-plane O–H bending of MFBA.

C-F vibrations

The adjacent atoms easily affect the C-F vibrations and therefore the band for stretching C-F vibrations[24] has been identified in the wavenumber range 1360-1000 cm^{-1}. The C-F mode stretching vibrations for IR spectra are observed at 1281, 1250 and 1189 cm^{-1} and Raman spectra at 1250 cm^{-1}, which matches with TED (72%). The out-of-plane and in-plane C-F vibrations are enumerated in the Table 2.

Prediction of First Hyperpolarizability

In the present study of MFBA, the field finite approach has been utilized for calculating the first hyperepolarizability (β) tensor represented as 3 x 3 x 3 matrix and 27 matrix terms into 10 components because of Kleinman symmetry[25]. The β term is described by Taylor series energy coefficients in the external electric field. If external electric field is homogeneous and weak, the expansion converts:

$$E = E_0 - \sum_i \mu_i F^i - \frac{1}{2}\sum_{ij} \alpha_{ij} F^i F^j - \frac{1}{6}\sum_{ijk} \beta_{ijk} F^i F^j F^k - \frac{1}{24}\sum_{ijkl} \nu_{ijkl} F^i F^j F^k F^l + \ldots$$

E_o unperturbed energy of the molecule; F^i represents field at origin, and μ_i, β_{ijk}, α_{ij} and ν_{ijkl} are the components corresponding to respective dipolemoment, first hyperpolarizabilities, polarizability, second hyperpolarizibilites. Average first

hyperpolarizability β, total dipole moment μ, average polarizability α by the components (x, y, z) are well-defined as,

$$\beta = \left[\left(\beta_{xxx} + \beta_{xyy} + \beta_{xzz}\right)^2 + \left(\beta_{yyy} + \beta_{xxy} + \beta_{yzz}\right)^2 + \left(\beta_{zzz} + \beta_{xxz} + \beta_{yyz}\right)^2 \right]^{1/2}$$

$$\mu = \left(\mu_x^2 + \mu_y^2 + \mu_z^2\right)^{1/2}$$

$$\overline{\alpha} = \frac{1}{3}\left(\alpha_{xx} + \alpha_{yy} + \alpha_{zz}\right)$$

$$\Delta\alpha = \frac{1}{\sqrt{2}}\left[\left[\left(\alpha_{xx} - \alpha_{yy}\right)^2 + \left(\alpha_{yy} - \alpha_{zz}\right)^2 + \left(\alpha_{zz} - \alpha_{xx}\right)^2 + 6\alpha_{xx}^2 \right] \right]^{1/2}$$

Table 3 reflects the calculated first hyperpolarizability, polarizability and dipolemoment components. The total dipolemoment, mean polarizability, first hyperpolarizability and anisotropic polarizability by DFT-B3LYP technique are 4.6834 Debye, 15.591 Å^3, 3.245×10^{-30} cm^5 e.s.u.$^{-1}$ and 35.596 Å^3, respectively, which are good comparable with reported values of urea[26]. Therefore, the first hyperpolarizability and dipolemoment of MFBA is 8.7 and 3.4 times larger than comparing with urea. We conclude that MFBA is a suitable choice for nonlinear optical (NLO) applications.

Table 3: Dipolemoment μ (Debye), first hyperpolarizability (β) and polarizability (α) components for 3-methoxy-2,4,5-trifluorobenzoic acid in atomic units

Components	Values	Components	Values
μ_x	-3.9891	β_{xxx}	-108.4396542
μ_y	-2.2532	β_{xxy}	-82.0431771
μ_z	-0.6493	β_{xyy}	-136.6689111
		β_{yyy}	-188.7373207
α_{xx}	133.3372535	β_{xxz}	-9.909462
α_{xy}	10.8829526	β_{xyz}	1.3497206
α_{yy}	121.3333575	β_{yyz}	-5.93585
α_{xz}	-9.9575474	β_{xzz}	13.2030282
α_{yz}	-2.7518548	β_{yzz}	-14 .616223
α_{zz}	61.2857676	β_{zzz}	-61.0082267

LUMO-HOMO band gap

The LUMO and HOMO[27] are the key factors in deciding the chemical stability of the molecule. As we known that LUMO and HOMO denotes the capability to accept and donate an electron, respectively. Fig. 4 shows 3D plots of LUMO and HOMO by B3LYP-6-311G++(d,p) method for MFBA. The energy gap between LUMO and HOMO of MFBA is 5.417 eV, which clarifies the interactions due to charge transfer occur in MFBA. The HOMO is mostly situated over the three fluorine atoms of MFBA and LUMO is sited over the COOH functional group. Therefore, the transition from HOMO to LUMO suggests the transfer of electron density to ring system of MFBA and COOH group from the three fluorine atoms (F11, F17 and F18).

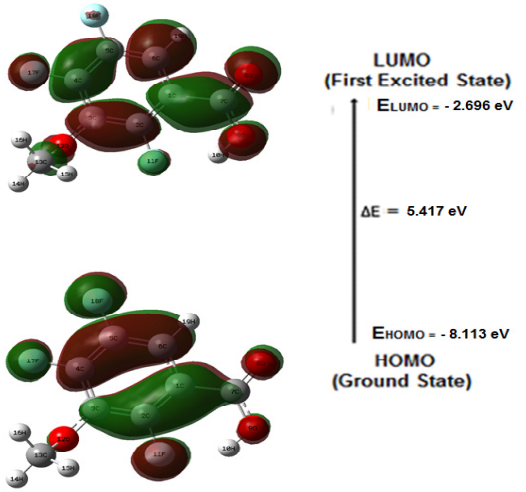

Fig. 4. Frontier orbital of 3-methoxy-2,4,5-trifluorobenzoic acid

Natural Bond Orbital (NBO) analysis

Natural Bond Orbital investigation explains about the conjugative interaction of the molecules. An interaction among the filled and virtual orbitals improves the examination of inter and intra molecular interactions[28]. The donor(i) and acceptor(j) interaction was explained using second-order Fock matrix. A donor can be occupied or lone pair orbital. But an acceptor can be an empty or occupied (both bond and antibond) or lone pair orbitals. The weaker or stronger bond depends on the interaction between the acceptor and donor. For each donor (i) and acceptor (j), the delocalized stabilization energy $E^{(2)}$ from i → j is projected as follows,

$$E_2 = \Delta E_{ij} = q_i \frac{F(i,j)^2}{e_i - e_j}$$

Here, ε_i and ε_j are crosswise elements, qi is the orbital donor occupancy and *F(i,j)* is the Fock diagonal matrix element. Larger the stabilization energy $E^{(2)}$, the more rigorous will be the donors and acceptors electron interaction and larger the degree of conjugation of entire system. NBO study of MFBA was achieved at DFT method (B3LYP-6-311G++(d,p)) so as to explicate the intra-molecule hybridization, conjugative charge transfers interaction and electron delocalization inside the molecule. The

perturbation analyses (2nd order) of NBO Fock matrix for MFBA are illustrated in Table 4. There is a strong n-π conjugation among the lone pair oxygen, fluorine electrons and π system (benzene ring). The orbital interaction in lone pair of oxygen atoms $n2(O_8)\rightarrow\sigma^*(C1–C7)$, $n2(O_9)\rightarrow\pi^*(C_7–O_8)$ and $n2(O_{12})\rightarrow\sigma^*(C_3–C_4)$ consequences stabilization energies15.40, 36.06 and 6.53 kJ mol^{-1}, respectively. These interactions show n-σ, n-π conjugation between oxygen atoms and the benzene ring. Similarly, the fluorine atoms leads the stabilization energies of 17.22, 18.95 and 18.14 kJ mol^{-1} for the interactions $n3(F_{11})\rightarrow\pi^*(C_2–C_1)$, $n3(F_{17})\rightarrow\pi^*(C_4–C_3)$ and $n3(F_{18})\rightarrow\pi^*(C_6–C_5)$, respectively. In MFBA molecule, the interesting interactions is $\pi^*(C_3\text{-}C_4)$ to $\pi^*(C_5–C_6)$ which result huge stabilization value 244.76 kJ mol^{-1}. This maximum interaction can encourage the large bioactivity around the ring of MFBA. Hence, the MFBA structure becomes stable through these interactions.

Table 4: NBO analysis for 3-methoxy-2,4,5-trifluorobenzoic acid

Donor (i)	ED (i) (e)	Acceptor (j)	ED (j) (e)	Interaction energyE(2) (kJ mol^{-1})	Energy (a.u.) difference E(j)–E(i)	Fock matrix element F (i,j) (a.u.)
$\sigma(C_1 – C_2)$	1.97691	σ*(C2 – C3)	0.03695	3.73	1.26	0.061
$\pi(C_1 – C_2)$						
	1.67114	π*(C3 – C4)	0.40950	19.55	0.28	0.067
		π*(C5 – C6)	0.35072	19.82	0.29	0.068
		π*(C7 – O8)	0.22853	15.40	0.29	0.061
$\sigma(C_1 – C_6)$	1.96486	σ*(C2 – F11)	0.02726	4.04	0.95	0.056
$\sigma (C_2 – C_3)$	1.97890	π*(C1 – C2)	0.03073	4.21	1.27	0.066
$\pi(C_3 – C_4)$	1.97751	π*(C1 – C2)	0.43157	19.96	0.29	0.070
		π*(C5 – C6)	0.35072	18.07	0.30	0.066
$\pi(C_5 – C_6)$	1.66259	π*(C1 – C2)	0.43157	19.49	0.28	0.067
		π*(C3 – C4)	0.40950	22.15	0.27	0.070
$\pi(C_7 – O_8)$	1.98113	π*(C1 – C2)	0.43157	4.56	0.35	0.040
$n2(O_8)$	1.84942	σ*(C1 – C7)	0.06872	15.40	0.61	0.088
		σ*(C1 – O9)	0.09666	29.20	0.51	0.110
$n2(O_9)$	1.83009	ϖ*(C7 – O8)	0.22853	36.06	0.31	0.096
$n2(F_{11})$	1.95337	π*(C2 – C3)	0.03695	6.93	1.03	0.076
		π*(O9 – H10)	0.02602	10.36	0.97	0.090
$n3(F_{11})$	1.93111	π*(C1 – C2)	0.43157	17.22	0.45	0.087
$n2(O_{12})$	1.93576	σ*(C3 – C4)	0.03604	6.53	0.82	0.066
		σ*(C13 – H14)	0.01495	5.15	0.73	0.055
$n3(F_{17})$	1.91968	π*(C3 – C4)	0.40950	18.95	0.41	0.087
$n3(F_{18})$	1.92375	π*(C5 – C6)	0.35072	18.14	0.42	0.084
$\pi^*(C_3 – C_4)$	0.40950	π*(C5 – C6)	0.35072	244.76	0.01	0.080

Thermodynamic Properties

The Table 5 shows the calculated values of different parameters (entropy, heat capacity and vibrational energy) at normal temperature by B3LYP method. The scaling factor has been suggested[29] for exact prediction to determine the entropy (S_{vib}) and zero-point vibration energies (ZPVE). The calculated total energy and vibrational energy of MFBA are 84.641 and 82.864 kcal mol^{-1}, respectively and the insignificant zero point vibrational energy is obtained (76.657 kcal mol^{-1}). These parameters can be utilized to estimate the order of chemical reactions and also for investigating different thermodynamic energies from thermodynamic relative functions.

Mulliken's Population Analysis

Figure 5 demonstrations the Mulliken's charges plot for MFBA from B3LYP larger basis set calculation. In the outcome, it is noticed that the fluorine atoms, COOH and methoxy groups leads to electron density redistribution in the MFBA ring system. The distribution of charge in the molecule has a greater impact on the vibrational spectra[30]. In comparison to carbon atoms in the ring, C1atom bonded with the COOH assembly have more positive charge (1.566), on the same way carbon C3 atom bonded with electron donating methoxy groups have negative charge (-0.3634). The atoms of carbon C2, C4 and C5 attached to fluorine atoms have small Mulliken charge values as shown in Figure 5.

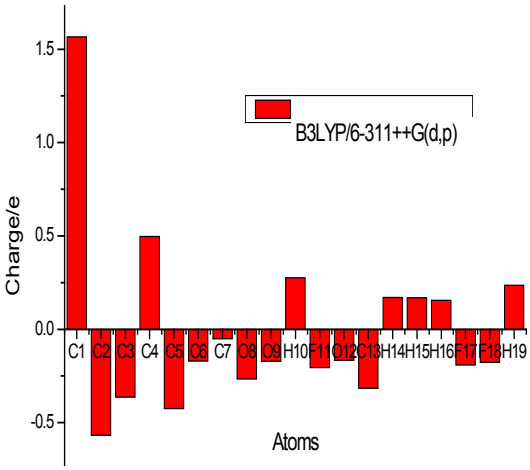

Fig. 5. Mulliken's charges plot of 3-methoxy-2,4,5-trifluorobenzoic acid

Table 5: Thermodynamic quantities of 3-methoxy-2,4,5-trifluorobenzoic acid

Parameters	Method-Basis set B3LYP-6-311++G(d,p)
Minimum optimized Energy in Hartrees	-833.276940748
$E_{\text{total thermal}}$ in kcal mol^{-1}	84.641
Heat capacity, C_v in cal mol^{-1} k^{-1}	45.911
Total Entropy, S in cal mol^{-1} k^{-1}	113.082
$S_{\text{Translational}}$ in cal mol^{-1} k^{-1}	41.873
$S_{\text{Rotational}}$ in cal mol^{-1} k^{-1}	31.801
$S_{\text{Vibrational}}$ in cal mol^{-1} k^{-1}	39.409
E_{vib} in kcal mol^{-1}	82.864
$E_{\text{zero point vib}}$ in kcal mol^{-1}	76.657
Rotational constants in GHz	
A	0.96520
B	0.55158
C	0.35796
Dipolemoment in Debye	4.6834

MEP Analysis

For MFBA, molecular electrostatic potential (MEP) analysis used to predict electrophilic and nucleophilic attack[31] by B3LYP method and in Fig. 6 the pictorial representation is shown. Negative electrostatic potential (ESP) spread over the COOH, methoxy functional groups is replicated as a yellowish spot and rest of the molecule contains the positive ESP. In the MEP diagram, the potential energy decreases from blue > green > yellow > orange > red. The MEP map on oxygen atoms (Red) of COOH group indicates the negative potential sites and around hygrogen atoms of the molecule (blue) represents positive potential sites. Furthermore, in MFBA, two concepts have been identified based on attraction and repulsion. The strongest attraction and repulsion are represented by hydrogen and oxygen atoms, respectively.

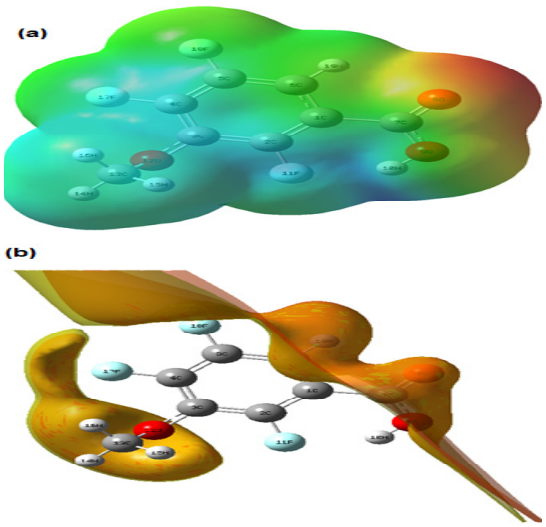

Fig. 6. (a) MEP; (b) ESP for 3-methoxy-2,4,5-trifluorobenzoic acid

CONCLUSION

The geometrical optimized parameters, band intensities and wave numbers for 3-methoxy-2,4,5-trifluorobenzoic acid was investigated using B3LYP larger basis set calculations together with the observed spectra. The experimental values match well through the results of DFT-B3LYP method. Influence of COOH, methoxy groups and fluorine atoms in the molecule is also discussed. Furthermore, studies on MFBA reveal as a good candidate for nonlinear optical study. LUMO-HOMO energy gap and NBO analyses explains the intermolecular transfer of charges in MFBA which are responsible for biological activity. The Mulliken charge analysis explains the electron concentration rearrangement. The MEP of MFBA expects the relative activity to nucleophilic (oxygen atoms) and electrophilic (hydrogen atoms) occurrences. These outcomes will be evidence for 3-methoxy-2,4,5-trifluorobenzoic acid in pharmaceuticals, food industries and electro optical studies.

ACKNOWLEDGEMENT

Facilities provided by Kalasalingam Academy of Research and Education, Krishnankoil are gratefully acknowledged.

Conflicts of Interest

None

REFERENCES

1. Warth, A. D. *Appl Environ Microbiol*., **1991**, *57*, 3410-3414.
2. Pollard, J. A; Russel, N. J; Gould, G. W. Food preservatives, (AVI Publishers: New York)., **1991**, 235.
3. Swinslocka, R; Samsonowicz, M.; Regulaska, E.; Lewandowski, W. *J. Mol. Struct*., **2006**, *792*, 227-238.
4. Sheldon, R. A.; Kochi, J. K. Metal-catalyzed oxidations of organic molecules, (Academic: New York)., **1981**.
5. Kreutz, K.; Schlossberg, A. *U S Patent*., **2002**, *6*,395-720 B1.
6. Karabacak, M.; Cinar, M. *Spectrochim. Acta Part A Mol. Biomol. Spectrosc*., **2012**, *86*A, 590-599.
7. Karabacak, M.; Cinar, Z.; Kurt, M.; Sudha, S.; Sundaraganesan, N. Spectrochim. *Acta Part A Mol. Biomol. Spectrosc*., **2012**, *85*A, 179-189.
8. Ramalingam, S.; Periandy, S. *Spectrochim. Acta Part A Mol. Biomol. Spectrosc*., **2011**, *78*A, 835-843.
9. Korth, H. G. De Heer, M. I.; Mulder, P. *J. Phys. Chem*., **2002**, *106*, 8779-8789.
10. Xavier, R. J.; Gobinath, E. Spectrochim. *Acta Part A Mol. Biomol. Spectrosc*., **2012**, *91*A, 248-255.
11. Becke, A.D. *J. Chem. Phys*.,**1993**, *98*, 5648–5652.
12. Frisch, M.J.; Trucks, G.W.; Schlegel, H.B.; Scuseria, G.E.; Robb, M.A.; Cheeseman, J.R.; Scalmani, G.; Barone, V.; Mennucci, B.; Petersson, G.A. GAUSSIAN 09, Revision A.02, Gaussian Inc, Wallingford CT., **2009**.
13. Lee, C.; Yang, W.; Parr, R.R. *Phys. Rev*.,**1988**, B *37*, 785–789.
14. Rauhut, G.; Pulay, P. *J. Phys. Chem*., **1995**, *99*, 3093-3100.
15. MOLVIB (V.7.0): Calculation of Harmonic Force Fields and Vibrational Modes of Molecules, QCPE Program No. 807., **2002**.
16. Gupta, M. P.; Prasad, S. N. *Acta Cryst*., **1971**, B*27*, 713-717.
17. Richard Betz, Thomas Gerber, *Acta Cryst*., **2011**, E*67*, 0539-0540.
18. Jeyavijayan, S. *Indian J. Pure Appl. Phys.,* **2016**, *54*, 269-278.
19. Sajan, D.; Hubert Joe I.; Jayakumar, V. S. *J. Raman. Spectrosc*., **2005**, *37*, 508-519.
20. SugirthaSuni N.Y.; GuruPrasad L; Ganapathi Raman R. *Orient. J. Chem*., **2018**, *34*(3), 1638-1645.
21. Socrates, G. Infrared and Raman characteristic group frequencies, (John Wiley: New York)., **2001**.
22. Coates, J. Interpretation of infrared spectra, a practical approach, in Meyers R A (Eds), Encyclopedia of analytical chemistry, (John Wiley & Sons Ltd: Chichester)., **2000**.
23. Sathyanarayana, D. N. Vibrational Spectroscopy Theory and Applications, second ed., New Age International (P) Limited Publishers, New Delhi., **2004**.
24. Venkata Ramana Rao, P.; Srishailam, K.; Ravindranath, L.; Venkatram Reddy, B.; Ramana Rao, G. *J. Mol. Struct*., **2019**, *1180*, 665-675.
25. Karpagam, J.; Sundaraganesan, N.; Sebastian, S.; Manoharan, S.; Kurt, M. *J. Raman Spectorsc*., **2010**, *41*, 53-62.
26. Sun, Y. X.; Hao, Q. L.; Wei, W. X.; Yu, Z. X.; Lu, L. D.; Wang, X.; Wang, Y. S. *J. Mol. Struct.,* (*Theochem*.)., **2009**, *904*, 74-82.
27. Padmaja, L.; Ravi Kumar, C.; Sajan, D.; Joe, I. H.; Jayakumar, V. S.; Pettit, G. R. *J. Raman Spectorsc*., **2009**, *40*, 419-425.
28. Prathipa, C.; Kalpana, P.; Akilandeswari, L. *Indian J. Chem*., **2018**, *57*A, 643-648.
29. Alcolea Palafox, M. *Int. J. Quant Chem*., **2000**, *77*, 661-684.
30. Gunasekaran, S.; Kumaresan, S.; Arunbalaji, R.; Anand, G.; Srinivasan, S. *J. Chem. Sci.,* **2008**, *120*, 315-324.
31. Murray, J. S.; Sen, K. Molecular Electrostatic Potentials, Concepts and Applications, Elsevier, Amsterdam., **1996**, 7–624.